https://doi.org/10.5194/mr-2021-51
Preprint. Discussion started: 15 July 2021

Open Access MAGNETIC RESONANCE Discussions

The relation between crystal structure and the occurrence of quantum-rotor induced polarization

Corinna Dietrich,[1] Julia Wissel,[1] Oliver Lorenz,[1] Arafat Hossain Khan,[2] Marko Bertmer,[2] Somayeh Khazaei,[3] Daniel Sebastiani,[3] Jörg Matysik[1]

[1]Institut für Analytische Chemie, Universität Leipzig, Linnéstr. 3, 04103 Leipzig, Germany

[2]Felix-Bloch-Institut für Festkörperphysik, Universität Leipzig, Linnéstr. 5, 04103 Leipzig, Germany

[3]Institut für Chemie, Martin-Luther-Universität Halle-Wittenberg, Von-Danckelmann-Platz 4, 06120 Halle, Germany

Correspondance: Jörg Matysik (joerg.matysik@uni-leipzig.de)

ABSTRACT

Among hyperpolarization techniques, quantum-rotor induced polarization (QRIP), also known as Haupt effect, is a peculiar one. It is on one hand rather simple to apply by cooling and heating of a sample. On the other hand, only the methyl groups of a few substances seem to allow for the effect, which strongly limits the applicability of QRIP. While it is known, that a high tunnel frequency is favorable, the structural requirements for the effect to occur are not exhaustively studied yet. Here we report on our efforts to heuristically recognize structural motifs in molecular crystals able to allow to produce QRIP.

https://doi.org/10.5194/mr-2021-51
Preprint. Discussion started: 15 July 2021

Open Access MAGNETIC RESONANCE Discussions

1 INTRODUCTION

NMR spectroscopy is a very versatile analytical method, however, caused by the low Boltzmann ratio, suffers from a lack of sensitivity. Therefore, hyperpolarization methods are presently a “hot” issue (Halse, 2016; Köckenberger and Matysik, 2010; Kovtunov et al., 2018; Wang et al., 2019). Examples of these techniques are dynamic nuclear polarization (Ardenkjaer-Larsen, 2016; Kjeldsen et al., 2018; Lilly Thankamony et al., 2017; Milani et al., 2015; Ni et al., 2013), spin-exchange optical pumping (Hollenbach et al., 2016; Meersmann and Brunner, 2015; Norquay et al., 2018; Walker, 2011), photochemically induced dynamic nuclear polarization (Bode et al., 2013; Kiryutin et al., 2012; Sosnovsky et al., 2019) and para-hydrogen induced polarization

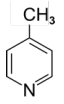

1

Figure 1: γ-picoline (**1**).

(Duckett and Mewis, 2012; Kiryutin et al., 2017; Korchak et al., 2009). Another technique is quantum-rotor induced polarization (QRIP) (Dumez et al., 2017; Horsewill, 1999; Icker et al., 2013; Icker and Berger, 2012; Ludwig et al., 2010). It was first observed by Haupt in γ-picoline (**1**, Figure 1) during rapid temperature jumps at very low temperatures (Haupt, 1972, 1973).

It is also possible to access the signal enhancement in liquid state, by freezing **1** at helium temperature and then rapidly dissolving it in deuterated solvents at room temperature and measuring it immediately (Icker and Berger, 2012). With a custom-made setup, we were able to improve the safety and speed of the dissolution and transfer process, resulting in a higher signal enhancement factor of 530 (Dietrich et al., 2018). An example of a QRIP enhanced spectrum is given in Figure 2. The enhancement is limited to the signal of the methyl carbon and exhibits a before unexpected antiphase pattern (Icker and Berger, 2012).
One might expect that more methyl bearing compounds allow for QRIP, which would broaden the applicability of the effect. However, work of Icker and Berger (Icker et al., 2013) indicated that only a few substances with methyl groups can be hyperpolarized in this way and all of the positively tested compounds show a weaker hyperpolarization compared to **1**. Therefore, the structural requirements for the occurrence of QRIP need to be elucidated.

https://doi.org/10.5194/mr-2021-51
Preprint. Discussion started: 15 July 2021

Open Access MAGNETIC RESONANCE Discussions

For a deeper understanding of these requirements, we discuss the underlying mechanisms of the effect. Thermodynamically, QRIP has been interpreted in terms of a resonant contact between a tunnelling reservoir and a Zeeman reservoir (Horsewill, 1999) at low temperatures. The nuclear spin-order is produced via coupling of spin-states to rotational quantum states of the methyl group. At the temperature of liquid helium only the lowest rotational state is occupied. Upon a dramatic temperature jump to room temperature, a measurable non-Boltzmann distribution of nuclear spin states is gained via cross-relaxation effects. These relaxations also explain the antiphase pattern and are further described in (Roy et al., 2013).

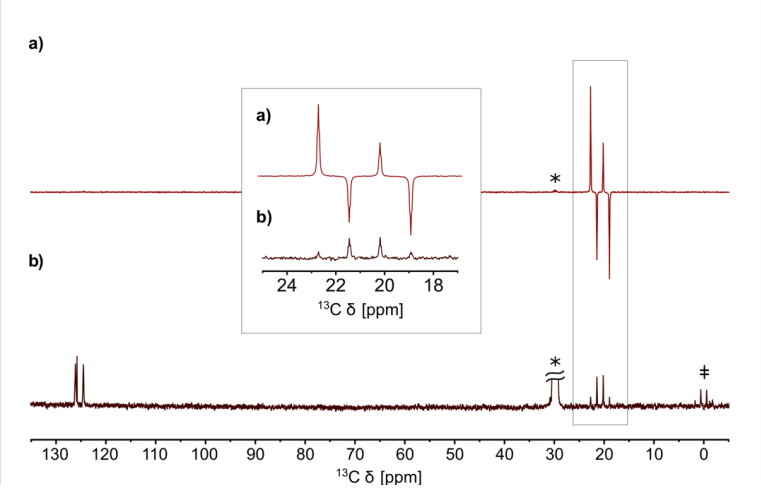

Figure 2: a) QRIP enhanced ^{13}C spectrum of γ-picoline (**1**) measured without proton decoupling, recorded with one scan after the cooling and dissolution procedure. Acetone-d6 was used as solvent. b) Reference spectrum recorded after full relaxation with 100 scans. The signals of acetone-d6 (labelled with asterix, *) and TMS (‡) are strongly visible in the reference spectrum.

The energy gap between the rotational ground state and the first excited state determines the (low-temperature) population ratio via the Boltzmann factor and thus the overall amplitude of the imposed spin symmetry constraint. Thus, it can be expected that high tunnel frequencies are strongly favorable for observing QRIP effects. In fact, **1** has an exceptionally high tunnel frequency of 520 μeV (~ 4 cm^{-1}) (Prager and Heidemann, 2010). The tunnel frequency is also linked to the capability of the methyl group to rotate freely (Barlow et al., 1992). Therefore, structural motifs with free methyl groups are especially interesting. In the case of **1**, the crystal structure shows a rather special feature. Each methyl group is paired with another one and the pairs are all aligned perfectly in a face-to-face manner. Around both methyl pairs, the chemical environment creates rotational potential energy barriers (often with a C_3 or C_6 symmetry). There is a strong coupling of both these methyl groups (due to their spatial proximity) with a $2\pi/6$ phase difference, which means that the superposition of the two rotational potential energy functions becomes surprisingly flat (i.e. the hills of the first rotational potential just fit to the valleys of the second potential function). This in turn leads to the possibility for joint rotation of the methyl groups at very low rotational barrier, virtually a free rotation, eventually resulting in a very high tunnel splitting (Khazaei and Sebastiani, 2017).

In the present work, we therefore search for substances which have one or several of these features: methyl groups with low steric hindrance, methyl groups in a similar distance to each other and face-to-face arrangement as in **1**, and methyl groups with concerted rotations.

https://doi.org/10.5194/mr-2021-51
Preprint. Discussion started: 15 July 2021

Open Access MAGNETIC RESONANCE Discussions

2 MATERIALS AND METHODS

2.1 Liquid-state NMR

Experiments were carried out on a Bruker Fourier-300 and a Bruker DRX-400 spectrometer. For the QRIP studies, samples were cooled for 90 min in liquid helium and subsequently mixed with deuterated solvents at room temperature. The mixture was transferred to the magnet and measured immediately. This procedure was carried out manually or with the self-built transfer system where the mixing and the transfer of the solution into the magnet is carried out in one step during 35 s (Dietrich et al., 2018). If suitable, the transfer system has been preferred, due to faster sample transfer into the magnet. In cases of insufficient solubility, solely the manual procedure has been found to be applicable. To validate structures and determine the signal enhancement factor, reference spectra were measured after full relaxation of the enhancement. Therefore, multiple scans were recorded, whereas QRIP enhanced spectra have been obtained with a single scan.

2.2 Solid-state NMR

For the solid-state experiments under magic-angle-spinning (MAS), a Bruker Avance III spectrometer (400 MHz ^{1}H frequency) was used. In order to test for QRIP enhancement, the powder sample was packed into a 4-mm zirconia rotor, closed with a zirconia cap and cooled for 90 min in liquid helium. After cooling, the rotor was transferred manually into the magnet and spectra were recorded. For the measurement under vacuum, the powder sample was filled into a glass tube (3 mm outer diameter) and evacuated over 2 days. Afterwards, the glass tube was sealed and fitted into the 4-mm zirconia rotor with polytetrafluoroethylene stoppers (Khan et al., 2018). The rotor was closed with a zirconia cap and used as before. In every case, non-decoupled Hahn echo pulse sequences were used and the spinning frequency was set to 8 kHz. Again, reference spectra with multiple scans were recorded afterwards.

2.3 Signal enhancement factor

To compare QRIP enhanced spectra with one scan to reference spectra with multiple scans, the enhancement factor ε has been calculated by using equation 1. $(S/N)_{QRIP}$ is the signal to noise ratio of the QRIP-enhanced signal and $(S/N)_{ref}$ is the signal to noise ratio of the reference spectrum with multiple scans. The number of scans is given as n_{ref} (Dietrich et al., 2018). *S/N* ratios were obtained from the Topspin 3.1 software.

$$\varepsilon = \frac{\sqrt{n_{ref}} \cdot (S/N)_{QRIP}}{(S/N)_{ref}} \quad (1)$$

2.4 Inelastic neutron scattering

Inelastic neutron scattering (INS) measurements were carried out at the TOF-TOF instrument at the Forschungs-Neutronenquelle Heinz Maier-Leibnitz (Garching, Technical University of Munich).

2.5 X-ray diffraction

For the powder X-ray diffraction (PXRD) patterns, the samples were placed in 0.5 mm Ø capillaries and measured using a STOE STADI P diffractometer (Cu $K\alpha_1$ radiation; equipped with a MYTHEN (DECTRIS) detector). Measurements were carried out at the Institute of Inorganic Chemistry, University of Leipzig.

2.6 Synthesis

γ-Picoline hydrochloride (**2**) was commercially available (Carbosynth Limited), while γ-picoline nitrate (**3**) and γ-picoline hydrosulfate (**4**) were synthesized according to instructions from (Wang et al., 2015) and (Ullah et al., 2015).

https://doi.org/10.5194/mr-2021-51
Preprint. Discussion started: 15 July 2021

Open Access MAGNETIC RESONANCE Discussions

3 EXPERIMENTAL RESULTS AND DISCUSSION

3.1 Chemical analogues of γ-picoline

To gain a better understanding of the conditions for the occurrence of the effect, this heuristic study aims at finding connections between the various structural properties of a substance and the observed signal enhancement by QRIP. First, molecules that are similar to **1** in their molecular structure were searched and as a result very close analogues, three different salts of **1**, were found (Figure 3).

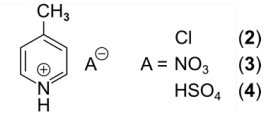

Figure 3: γ-picoline derivatives **2**-**4**.

All salts are solids at room temperature and are soluble in H_2O. Hence, D_2O was used as solvent for the liquid-state NMR experiments. For the QRIP experiments, the manual transfer was chosen, since the high viscosity of D_2O hinders the liquid flow in the transfer system and results in air bubbles in the NMR tube inside the magnet which will lead to a disturbed signal. From each salt, 50 μmol were cooled for 90 min at 4.2 K, quickly dissolved in D_2O, the solution (inside the NMR tube) was shortly held in an ultrasonic bath to remove air bubbles and then transferred and measured. Even though the chemical structure and especially the chemical environment of the methyl group seem similar to **1**, no QRIP enhancement was observed for any of the three salts **2** to **4** in the ^{13}C NMR spectra. The ^{13}C NMR reference spectra are similar to the one of **1**, with slight chemical shift changes (see Table 1).

Table 1: ^{13}C NMR reference spectra of γ-picoline and its derivatives recorded on a Bruker Fourier-300 spectrometer. D_2O was used as solvent. The chemical shifts are given in ppm.

substance	assignment			
	C—CH_3	N=**C**H—CH	CH—**C**H=C_q	**C**H_3
γ-picoline (**1**)	152.5	150.9	128.0	23.0
γ-picoline hydrochloride (**2**)	161.7	140.0	127.9	21.9
γ-picoline nitrate (**3**)	164.4	142.8	130.6	24.5
γ-picoline hydrosulfate (**4**)	164.5	142.8	130.7	24.5

Remarkably, also other chemical analogues, like the α-form and the β-form of picoline, show no signal enhancement as was shown already before in the work of M. Icker et al. (Icker et al., 2013). They also have studied toluene (**5**), which is in its chemical structure very similar to **1** and shows little QRIP enhancement. Hence, we conclude that not the molecular structure is decisive for successful induction of QRIP and that already small modifications of the molecular structure can decide upon either QRIP induction or quenching.

https://doi.org/10.5194/mr-2021-51
Preprint. Discussion started: 15 July 2021

Open Access MAGNETIC RESONANCE Discussions

Searching for other parameters controlling the occurrence of QRIP, we recognize that lithium acetate dihydrate (**6**), which is no picoline analogue, shows moderate QRIP enhancement (weaker than **1**, stronger than **5**). Comparing the crystal structures, we found that both **1** and **6** exhibit pairs of methyl groups facing each other in a 180° angle (Figure 4 a and c), crystal structures from (Galigné et al., 1970; Ohms et al., 1985)), while the

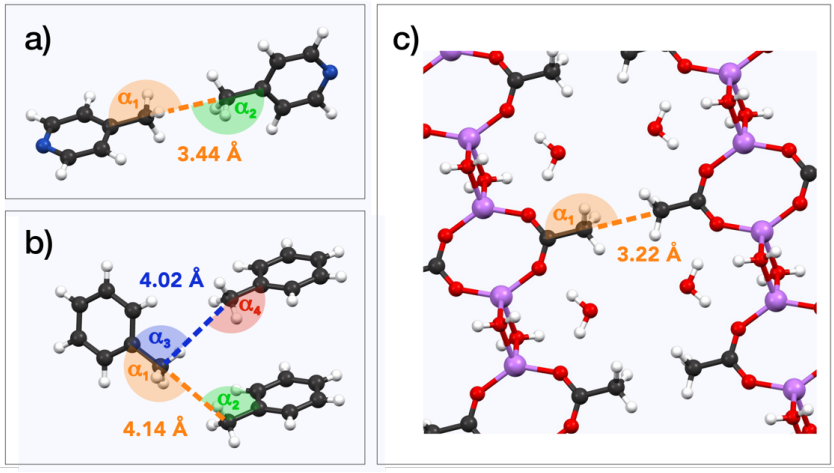

Figure 4: Examples for methyl pairs in the crystal structure. The distance between methyl pairs is given by the carbon-to-carbon distance. Angles are measured along the path from quaternary carbon via methyl carbon to the methyl carbon of the neighbor molecule. a) γ-Picoline (**1**) methyl pairs from crystal structure ZZZIVG, angles α_1 and α_2 vary between 177° and 180° (Ohms et al., 1985). b) Toluene (**5**) methyl pairs (TOLUEN), the distance between the closest pairs is either 4.02 Å or 4.14 Å. Respective angles: $\alpha_1 = 165°$, $\alpha_2 = 97°$, $\alpha_3 = 94°$, $\alpha_4 = 157°$ (van der Putten et al., 1990). c) Methyl pairs of lithium acetate dihydrate (**6**, LIACET), the angle α_1 is 180° (Galigné et al., 1970). The ionic bonds ($Ac^- \cdots Li^+ \cdots OH_2$) are plotted the same as regular covalent bonds in order to improve the spatial comprehensibility of the crystal representation.

methyl groups in **5** have no such symmetry (Figure 4 b), crystal structure from (van der Putten et al., 1990)). This might explain the different tunnel frequencies, which directly affect QRIP (see Table 2) (Icker et al., 2013; Roy et al., 2013). Since there is hardly "empty" space in condensed phase, in most crystal structures methyl groups cannot rotate freely. Only the direct compensation of two rotational barriers of two methyl groups which show a 180° face-to-face arrangement allows for almost "frictionless" rotations of the coupled methyls ("concerted" rotations, (Khazaei and Sebastiani, 2017)). Therefore, such a spatial arrangement in the crystal might provide a rare but well-defined structural feature allowing for induction of QRIP.

Table 2: Comparison of structural properties and QRIP: methyl-methyl- (Me-Me-) distances were measured carbon to carbon, angles between methyl groups were measured along the path from quaternary carbon via methyl carbon to the methyl carbon of the neighbor molecule (received from crystal structure data (Faber et al., 1999; Galigné et al., 1970; Ohms et al., 1985; van der Putten et al., 1990)); tunnel frequencies from (Prager and Heidemann, 2010) and QRIP signal enhancement factor ε from (Icker et al., 2013). Additionally to the name of the substance, the crystal structure code is given in parentheses.

substance (structure code)	Me-Me-distance [Å]	Me-Me-angle	tunnel frequency [μeV (cm^{-1})]	QRIP ε
γ-picoline (**1**, ZZZIVG)	3.44	177°-180°	520 (~ 4)	60
γ-picoline hydrochloride (**2**, DICCEX)	6.31	99°	-	-
toluene (**5**, TOLUEN)	4.02/4.14	94°-165°	28.5/26.0 (~ 0.2)	3
lithium acetate dihydrate (**6**, LIACET)	3.22	180°	250 (~ 2)	20

https://doi.org/10.5194/mr-2021-51
Preprint. Discussion started: 15 July 2021

Open Access MAGNETIC RESONANCE Discussions

The present work aims for further corroborating the experimental evidence of this correlation. Hence, our next step has been the systematic search for substances, which have structural properties similar to γ-picoline (**1**) in regards to the methyl-methyl distance and the face-to-face arrangement of the methyl groups. To this end, we searched for compounds of matching crystal structures.

3.2 Systematic crystal structure search

To find promising candidates for QRIP signal enhancement, the Cambridge Crystallography Database was searched for substances with similar distances and angles between methyl groups compared to those values given in Table 2. Other desired properties were relatively small molecular size (to have a high methyl concentration and better chances to observe signal) and commercial availability. All six selected substances are listed in Table 3.

Table 3: investigated compounds **7**-**12** from the systematic crystal structure search. Methyl-methyl- (Me-Me-) distances were measured carbon to carbon, angles between methyl groups were measured along the path from quaternary carbon via methyl carbon to the methyl carbon of the neighbor molecule. The crystal structure data was obtained from the Cambridge Crystallography Database. Additionally to the name of the substance, the crystal structure CODE is given in parentheses.

substance (structure code)	molecular structure	Me-Me-distance [Å]	Me-Me-angle
N-(*p*-tolyl)acetamide (**7**, ACTOLD)	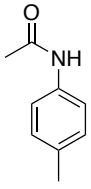	3.61	153°/170°
2,5-dimethyl-1,3-dinitrobenzene (**8**, AYOYAP)	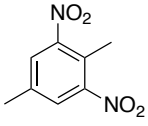	3.55	168°
N-(*tert*-butyl)acetamide (**9**, APUYIU)	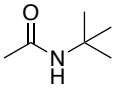	3.58	161°
Ethyl carbamate (**10**, ECARBM)	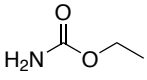	3.53	171°
2-nitropropane (**11**, IHIKIV)		3.23/3.46	90°-150°
N'-(3,4-difluorobenzylidene)-4-methylbenzenesulfonohydrazide (**12**, NUQDUA)	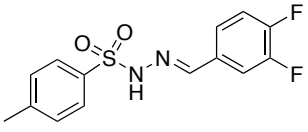	3.60	172°

https://doi.org/10.5194/mr-2021-51
Preprint. Discussion started: 15 July 2021

Open Access MAGNETIC RESONANCE Discussions

Although distances and angles between methyl groups of those compounds are in the range between compounds **1** and **5**, none of these compounds show a perfect face-to-face alignment of the methyl groups, and no QRIP enhancement was observed for any of them. The most probable reason is the occurrence of steric hindrance around the methyl groups in the crystal packing. This might affect the free rotation of the methyl

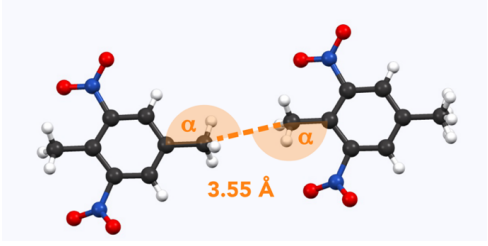

Figure 5: Example for methyl pairs in the crystal structure of **8** (AYOYAP) (Johnston and Crather, 2011). The distance between them is 3.55 Å (measured carbon to carbon). Respective angles (measured carbon to carbon to carbon): α = 168°.

groups, and, thus lead to lower tunnel frequencies inhibiting QRIP. Despite similar angles and distances of methyl groups, the impact of steric effects of the whole structure is difficult to estimate. To validate this correlation, theoretical calculations as in (Khazaei and Sebastiani, 2016, 2017) and experimental measurements of tunnelling frequencies are desirable. Another limitation can be a low concentration of methyl groups. In case

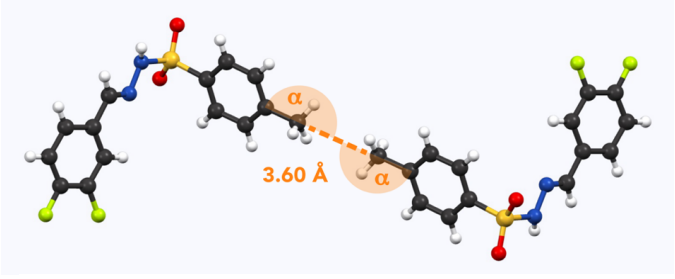

Figure 6: Example for methyl pairs in the crystal structure of **12** (NUQDUA) (Wang and Yan, 2015). The distance between them is 3.60 Å (measured carbon to carbon). Respective angles (measured carbon to carbon to carbon): α = 172°.

of low QRIP (as exhibited in **5**), higher amounts of the sample were necessary to observe a QRIP enhanced signal, i.e. 150 μmol for a good signal, whereas for **1** 50 μmol are sufficient to observe an intense QRIP enhanced signal. For compounds **7** to **11**, depending on the solubility between 50 and 100 μmol substance were used and in the case of **12** only 30 μmol was suitable.

https://doi.org/10.5194/mr-2021-51
Preprint. Discussion started: 15 July 2021

Open Access MAGNETIC RESONANCE Discussions

Compounds **8** and **12** were further investigated, since they were the 2 most promising candidates of this series. Interestingly, their methyl groups are in almost perfect face-to-face alignment (see Figure 5 (Johnston and Crather, 2011) and Figure 6 (Wang and Yan, 2015)). On the other hand, they differ in the alignment of the attached phenyl rings compared to **1**. While the phenyl rings of two molecules lie in the same plane for **8** and **12**, they are tilted 90° to each other in case of compound **1** (Figure 4 a)). Whether this structural difference has an impact on QRIP requires further theoretical investigations. To rule out that the obtained substances are amorphous or possess another crystal structure as compared to the literature, we performed X-ray diffraction (XRD) and confirmed the correct crystal structure of compounds **8** and **12** (Figure 7 and Figure 8).

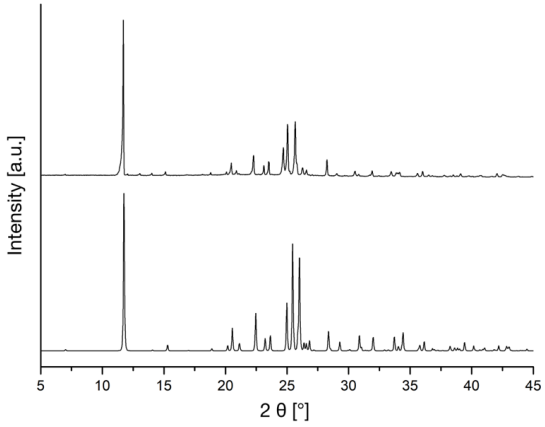

Figure 7: XRD spectra of **8**. Top: experimental data , bottom: simulated spectrum from crystal structure data (Johnston and Crather, 2011).

Furthermore, the tunnel frequency has been investigated by inelastic neutron scattering (INS). A multi-peak fit allowed to determine the first two transitions for each compound. For compound **8** we determined values of 40±10 μeV and 150±10 μeV (0.3 cm^{-1} and 1.2 cm^{-1}). For compound **12** we found 50±10 μeV and 160±10 μeV

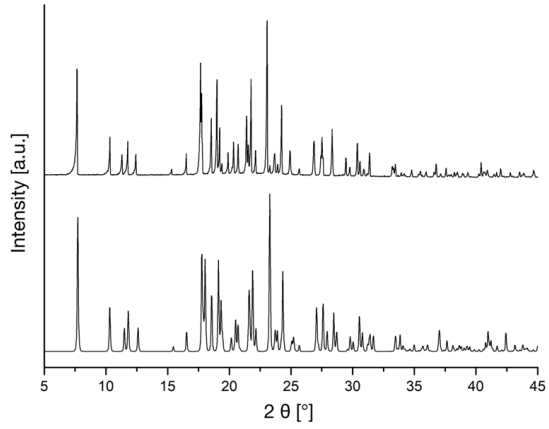

Figure 8: XRD spectra of **12**. Top: experimental data , bottom: simulated spectrum from crystal structure data (Wang and Yan, 2015).

(0.4 cm^{-1} and 1.3 cm^{-1}). These values lie in the range between the tunnel frequencies of **5** and **6** (26/28 μeV and 250 μeV), which both exhibit QRIP enhancement, but to a lower extent than **1**. Therefore, in regards to the tunnel frequencies, QRIP in compounds **8** and **12** is conceivable but very likely to exhibit only a weak enhancement.

https://doi.org/10.5194/mr-2021-51
Preprint. Discussion started: 15 July 2021

Open Access MAGNETIC RESONANCE Discussions

It is noteworthy, that in **8** each molecule possesses 2 methyl groups, thus the methyl concentration is higher compared to tests on **1** and is not expected to be the limitation. On the other hand, steric hindrance due to the NO_2 groups in close proximity to the methyl group might limit QRIP. In the case of **12**, there is no such hindrance through intramolecular factors, however, intermolecular hindrance is conceivable and the low concentration (30 μmol) is the most probable limitation.

3.3 Aspirin

Next to the crystallographic databank approach, we searched for compounds having a particularly low frequency mode of the methyl group. In its crystal structure, aspirin (acetylsalicylic acid, **13**) has a particularly low frequency mode near 30 cm^{-1} (3.7 meV), attributed to the concerted motions of methyl groups (Reilly and Tkatchenko, 2014). Compound **13** became an object of interest, since it exhibits some similarity to the compound **1**, in which the collective coupled motions of methyl groups are contributing to QRIP and the calculated methyl rotational barrier height of **1** is about 3.57 me (Khazaei and Sebastiani, 2016). Analysing the crystal structure of **13**, we found no face-to-face methyl pairs (ACSALA (Arputharaj et al., 2012)). The closest methyl pairs are in a distance of 4.43 Å to each other and the angles between them are 100°/147°. Multiple dissolution experiments showed no QRIP enhancement. According to (Prager and Heidemann, 2010), the tunnel frequency of **13** is 1.22 μeV (0.01 cm^{-1}), which is much lower than the tunnel frequencies of **1** and **2** (see Table 2). In fact, the mere coupling between two methyl groups (be it via a face-to-face arrangement or via lateral coupling similar to a cogwheel couple) is not sufficient for allowing a free rotation (leading to high tunnel splittings). A mandatory additional condition is that the rotational barriers created by the crystal surroundings have just the correct offset to each other. Assuming the common C_n symmetries for the rotational barriers, this means that the maximum of the rotational potential for one of the methyl groups has to coincide exactly with the minimum of the rotational potential of the other one. This additional condition seems to be not fulfilled for aspirin, leading to the absence of QRIP enhancement.

3.4 Calixaren complexes

Furthermore, we considered two types of compounds following our “chemical intuition”: calixarene compounds and metal-organic frameworks. Calixarenes can occur in a cone shape and are therefore able to host smaller molecules like toluene (Gutsche, 1981). Because of the highly symmetric structure inside the calixarene cone, we suspected a favourable situation for the methyl group of the guest toluene molecule to rotate freely. Thus, there might be a possibility to observe QRIP enhancement in this complex. Hence, we tested two calixarenes as hosts: calix[4]arene (**14**) and 4-*t*-butylcalix[4]arene (**15**) (see Figure 9).

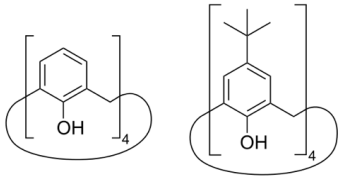

14 **15**

Figure 9: Structures of calix[4]arene (**14**) and 4-t-butylcalix[4]arene (**15**).

Complexes toluene@calix[4]arene (**16**) and toluene@4-*t*-butylcalix[4]arene (**17**) were synthesized by mixing a surplus of toluene with each calixarene at room temperature and letting the excess liquid dry (Andreetti et al., 1979).

In both cases, we did not succeed to obtain a sufficiently high concentration in solution in order to perform QRIP experiments. This is due to the weak solubility of the calixarene complexes in $CDCl_3$, acetone-d6 and toluene-d8, often resulting in opaque solutions or white suspensions with precipitate even for low concentrations. For compound **16** the solubility is higher than for **17**. In the best case, we achieved an almost clear solution of 20 mg of **16** in $CDCl_3$. Due to the higher mass of the complex in comparison to **1**, the resulting concentration is below what we expect to be observable by means of QRIP with the current setup. In future

https://doi.org/10.5194/mr-2021-51
Preprint. Discussion started: 15 July 2021

Open Access MAGNETIC RESONANCE Discussions

studies, calixarene complexes might be studied by solid-state NMR, avoiding the solubility issue. Furthermore, complexes with rather soluble calixarenes (Rehm et al., 2009) might provide an opportunity.

3.5 Metal Organic Frameworks (MOFs)

Compared to molecular crystals, MOFs provide an alternative approach to observe freely rotating methyl groups. Methyl groups with low steric hinderance are, for example, expected in MOFs such as ZIF-8 and ZIF-67 (zeolitic imidazole framework, see Figure 10). The difference in these two compounds lies in the different metal centre atoms: Zn(II) in ZIF-8 and Co(II) in ZIF-67. Due to the specific structure allowing for pore formation, the methyl groups are pointing toward the center of these pores and thus can rotate freely, which has been shown at cryogenic temperatures (Li et al., 2018; Zhou et al., 2008).

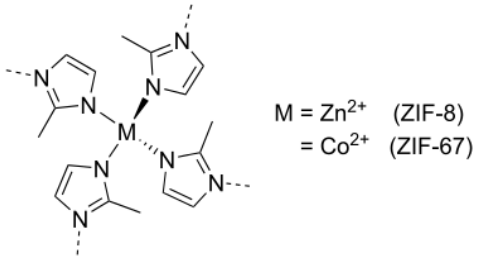

Figure 10: Structure of probed MOFs: ZIF-8 and ZIF-67.

Due to the low solubility and in order to avoid hindrance of free rotating methyl groups by solvent molecules inside the pores, the measurements were carried out in solid-state NMR. To ensure that carbon signal of both samples can be observed in general, reference spectra were recorded before and after the QRIP experiments. Examples of these spectra are given in Figure 11. The assignments of the signals are given in Table 4.

Table 4: ^{13}C NMR reference spectra of ZIFs recorded on a Bruker Avance III spectrometer (400 MHz ^{1}H frequency, solid-state NMR). The chemical shifts are given in ppm.

substance	assignment		
	N—**C**(CH_3)=N	N—**C**H=**C**H—N	**C**H_3
ZIF-8	143.4	128-110	17-7
ZIF-67	143.3	130-110	17-7

https://doi.org/10.5194/mr-2021-51
Preprint. Discussion started: 15 July 2021

Open Access MAGNETIC RESONANCE Discussions

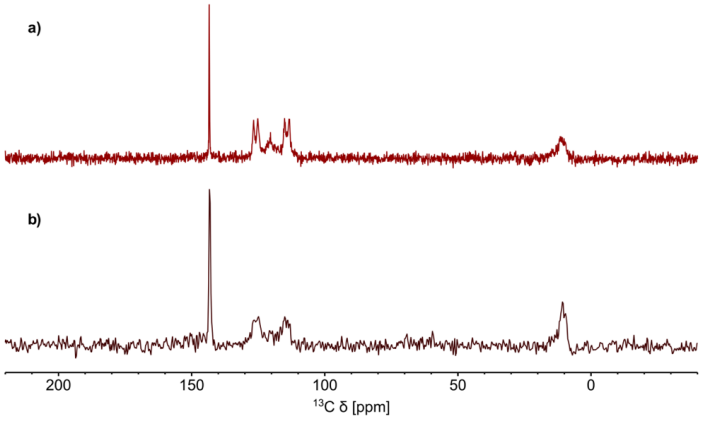

Figure 11: a) Spectrum of ZIF-8 measured in glass tube inside rotor. Hahn echo pulse sequence, non-decoupled, 8 kHz MAS frequency, 10.000 scans. b) Spectrum of ZIF-67 measured with regular packing method. Hahn echo pulse sequence, non-decoupled, 8 kHz MAS frequency, 1.000 scans.

In both cases, ^{13}C QRIP experiments were performed under MAS-conditions. The resulting spectra showed no signal enhancement. A possible explanation for the absence of QRIP can be the adsorption of air molecules inside the pores of the ZIFs (Moggach et al., 2011), which might hinder the free rotation of the methyl groups. To exclude this, subsequent measurements under vacuum were performed. Also in this case, both ZIF samples did not show QRIP.

It is noteworthy, that Co(II) is paramagnetic and hence, signal broadening and otherwise unexpected chemical shifts (Bertini et al., 2005; Gueron, 1975; Vega and Fiat, 1976) were expected. However, the obtained spectrum (Figure 11 b) shows no significant difference in the chemical shift in comparison to the Zn(II) analog (Figure 11 a). The signals are slightly broadened. Furthermore, an especially narrow line (20 Hz for ZIF-8, and 74 Hz for ZIF-67) at the far left of the spectrum is observed. The ^{13}C MAS NMR spectra were recorded without proton-decoupling since decoupling is expected to interfere with the QRIP effect. Therefore, CH and CH_3 signals of the ZIFs are broad, while the quaternary carbon is less affected. For the latter the closest proton is the one from the methyl group with a distance between the quarternary carbon and the methyl proton of 2.14 Å for ZIF-8 and 2.06 Å for ZIF-67. From this distance we calculated a CH-dipole-dipole coupling of 3083 Hz (ZIF-8), 3456 Hz (ZIF.67), which is averaged out at the chosen spinning speed of 8 kHz. With this and the high structural symmetry, resulting in a low chemical shift anisotropy, the narrow line can be explained.

For both ZIFs reference spectra with reasonable signal intensity were recorded after 1.000 scans for the regular packing method and 10.000 scans for the advanced packing method with glass tubes. Following equation 1 the signal enhancement factor ε should be at least 32 (regular packing, or 100 for advanced packing) in order to observe signal with one scan. Smaller signal enhancement via QRIP is conceivable but could not be observed with the current setup. An intrinsic limitation to QRIP might be the proximity between the methyl groups inside the pores (ZIF-8: 5.0 Å, crystal structure data from (Morris et al., 2012); ZIF-76: 4.6 Å (Kwon et al., 2015); measured from carbon to carbon). This might also lead to the absence of signal. Considering the broad variety of MOFs, it is conceivable, that some of them bear methyl groups, which rotate more freely or undergo concerted rotations, which are accessible for QRIP (Gangu et al., 2016; Gonzalez-Nelson et al., 2019; Kuc et al., 2007; Tarasi et al., 2020; Tian et al., 2007).

3.6 Analysis of previous data

Aiming for heuristic data on the relation between structure and the hyperpolarization obtained by QRIP, we revisited the crystal structures of compounds studied in (Icker et al., 2013) and (Icker, 2013). From all substances which were available in the Cambridge Crystallography Database, angles and distances between methyl pairs were extracted. Here, we searched specifically for methyl pairs with a similar distance as found

https://doi.org/10.5194/mr-2021-51
Preprint. Discussion started: 15 July 2021

Open Access MAGNETIC RESONANCE Discussions

in **1** (3.44 Å) and excluded all methyl pairs with a distance > 4.4 Å. The results are given in Table 5. If available, the tunnel frequencies (Prager and Heidemann, 2010) were included to Table 5 as well. Interestingly, many methyl pairs with a distance in the range 3.45-4.37 Å were found, which is quite similar to **1** and makes methyl coupling conceivable. On the other hand, no other face-to-face methyl groups were found. Angles close to 180° do not seem to be a sufficient argument to predict QRIP enhancement, as the comparison of two of the compounds shows: while **24** exhibits an 174° angle at a methyl-methyl distance of 4.06 Å it yields only a week polarization. Furthermore, a rather strong QRIP effect is observed in **25** where the most promising methyl pair has similar distance (3.78 Å), however, at the same time, it is less aligned with angles of 142°/158°. The surprisingly high polarization in **25** is still below **1** but larger than in **6** which is particularly curious since both **1** and **6** exhibit face-to-face methyl groups, while **25** does not. Although the structure of **25** does not fit our assumptions to gain QRIP, the tunnel frequency is surprisingly high, which fits the presence of QRIP.

It is possible, that the occurrence of multiple methyl groups in one molecule and multiple methyl pairs in the crystal structure are favourable for the likelihood of concerted rotations. However, those structural factors alone are also not sufficient for the prediction of QRIP, as other not or less polarizable substances like **7**-**9** (multiple methyl groups) contradict a general trend.

Table 5: List of compounds tested for QRIP in (Icker et al., 2013) and (Icker, 2013). Methyl methyl distances and angles between methyl groups were measured from the crystal structure data. Tunnel frequencies were taken from (Prager and Heidemann, 2010). Additionally to the name of the substance, the crystal structure CODE is given in parentheses.

substance (structure code)	Me-Me-distance [Å]	Me-Me-angle	tunnel frequency [μeV (cm^{-1})]	QRIP ε
sodium acetate (**18**, BOPKOG)	4.24 3.45	123°/142° 90°	1.5 (~ 0.01)	low
acetonitrile (**19**, QQQCIV)	3.95	139°	-	low
acetone (**20**, HIXHIF)	3.76 3.91	133°/176° 132°/158°	0.4 (~ 0.003)	low
α-picoline (**21**, ZZZHKQ)	4.09	63°/152°	-	0
p-xylene (**22**, ZZZITY)	3.71 4.14	90°/160° 99°	0.97 (~ 0.008)	0
p-cresol (**23**, CRESOL)	4.01	95°/113°	-	0
m-cresol (**24**, MCRSOL)	3.99 4.06 3.89 3.94	79°/176° 174° 83° 83°/114°	-	low
1,3-dibromo-2,4,6-trimethylbenzene (**25**, EJEROA)	3.77 3.78 4.08 3.74 4.03	134° 142°/158° 129°/156° 80°/83° 99°	390 (~ 3.1)	28
2-methoxynaphthalene (**26**, SAYRIT)	3.60 4.05 4.21	66°/172° 73°/107° 125°	-	0
2,6-di-*t*-butylnaphthalene (**27**, KOKQUW)	3.75 3.95 4.28	155°/161° 109°/124° 106°/136°	-	0
cholesterol (**28**, CHOEST)	4.37 4.31 4.31 3.56	98°/138° 91°/148° 89°/115° 84°/108°	-	0

https://doi.org/10.5194/mr-2021-51
Preprint. Discussion started: 15 July 2021

Open Access MAGNETIC RESONANCE Discussions

4 CONCLUSIONS

The aim of this study was to gain further understanding of the structural requirements of substances allowing for QRIP signal enhancement in NMR spectroscopy. Starting from the well-studied compound **1** we found that its derivatives (**2**-**4**) do not exhibit QRIP. This indicates that structural similarity on a molecular level is insufficient for QRIP prediction. The weak polarization in **5** and absence of QRIP in α-picoline and β-picoline (Icker et al., 2013) support this lack of correlation.

To better understand the specialty of **1**, we studied the crystal structure and recognized a rare structural feature: in its crystal structure pairs of methyl groups are aligned in a perfect 180° face-to-face manner. For the underlying tunnel effects freely rotating methyl groups and high tunnel frequencies are favorable. Via concerted rotations the face-to-face methyl groups in **1** can rotate exceptionally frictionless, like interacting gear wheels (Khazaei and Sebastiani, 2017; Roy et al., 2013).

In order to investigate the predictability and applicability of QRIP, we therefore searched for substances which show one or multiple of the aforementioned qualities: free rotation, promising alignment, high tunnel frequency of the methyl group, or concerted rotations of methyl groups. Thus, different approaches were tested.

First, we searched for compounds with similar methyl-methyl distances and angles as in **1** and found substances **7**-**12**. While all of them exhibit similar distances between methyl groups, they have no face-to-face arrangement of methyl groups and showed no QRIP enhancement. We conclude that either steric hindrance or missing positive interference of the methyl group is quenching the effect due to the less favorable arrangement.

Next, aspirin (**13**) was tested since it is described to have concerted motions of methyl groups. However, no QRIP enhancement was observed. We conclude that concerted rotations alone are insufficient. An additional condition is that the rotational barriers created by the crystal surroundings have just the correct offset to each other. This means that the maximum of the rotational potential for one of the methyl groups has to coincide exactly with the minimum of the rotational potential of the other one.

We further suspect freely rotating methyl groups in complexes of toluene in calixarene cones and in MOFs. While the free rotation in calixarene complexes derives from a very symmetric surrounding of the methyl group the MOFs show methyl groups in a relatively empty space. To this end, we did not succeed to perform QRIP measurements on calixarene complexes, due to its low solubility. In MOFs we did not observe QRIP enhancement.

Finally, we revisited previously studied compounds from (Icker et al., 2013) and compared QRIP enhancement to methyl-methyl distances and angles. In the analyzed crystal structures of **18**-**28** we found no face-to-face methyl groups, but a variety of angles and distances between methyl pairs. However, no general trend or correlation between distances/angles and the enhancement factor was found. On the contrary, we found that **25** shows a higher polarization than **6**, despite the missing face-to-face arrangement. Although we were not able to recognize structural patterns in the crystal structures related to the appearance of QRIP, we confirm that a high tunnel barrier is required to induce QRIP.

To explain why promising candidates like **8** and **12** showed no QRIP and **6** exhibits weaker QRIP than **1** (both show face-to-face methyl groups only with a slight difference in the methyl-methyl distance) we conclude that similarly as in **13** the necessary offset between rotational barriers of the methyl group is not given and thus QRIP is quenched. To summarize we find with this study that even small structural differences can quench the QRIP effect by strongly affecting the tunnel frequency. Thus, a broader applicability of the effect on, for example, protein methyl groups is not to be expected.

https://doi.org/10.5194/mr-2021-51
Preprint. Discussion started: 15 July 2021

Open Access MAGNETIC RESONANCE Discussions

Data availability. NMR spectra were originally recorded with TopSpin and processed with MestraNova. The TopSpin files include the raw data as well as the pulse sequences. Those files and the XRD data (Origin files) are available from zenodo.org with https://doi.org/10.5281/zenodo.5078040.

Supplement. The Supplement contains the following information: spectra of γ-picoline derivatives, crystal structure of γ-picoline hydrochloride and pictures of the glass tubes for MAS-NMR under air exclusion. The supplement related to this article is available online at: xxxxxx.

Author contributions. JM and DS designed the research. JW synthesized the γ-picoline derivatives. AHK prepared the glass tube samples for MAS-NMR under air exclusion. CD, JW and OL carried out the NMR measurements and CD, JW, OL, JM and DS interpreted the data. The paper was written with contributions from all the authors. All authors approved the final version of the paper.

Competing interests. The authors declare that they have no conflict of interest.

Special issue statement. This article is part of the special issue “Jeffery Bodenhausen Festschrift”. It is not associated with a conference.

Acknowledgements. The authors thank Prof. Dr. Stefan Berger, Dr. Maik Icker and Dr. Matthias Findeisen (Leipzig University) for helpful discussions. We also thank Dr. Astrid Schneidewind and Dr. Wiebke Lohstroh (Ludwig Maximilian University of Munich) for the INS measurements, and Oliver Erhart (Leipzig University) for the XRD measurements. Furthermore, we thank Dr. Michael Ruggiero (University of Vermont) for providing us with the ZIF-8 and ZIF-67 samples and Prof. Berthold Kersting und Dr. Peter Hahn (Leipzig University) for providing the calixarene samples.

Financial support. This work was supported by the Deutsche Forschungsgemeinschaft (DFG) under Grant number MA 4972/5-1.

REFERENCES

Andreetti, G. D., Ungaro, R. and Pochini, A.: Crystal and molecular structure of cyclo{quater[(5-t-butyl-2-hydroxy-1,3-phenylene)methylene]} toluene (1 : 1) clathrate, J. Chem. Soc. Chem. Commun., (22), 1005, doi:10.1039/c39790001005, 1979.

Ardenkjaer-Larsen, J. H.: On the present and future of dissolution-DNP, J. Magn. Reson., 264, 3–12, doi:10.1016/j.jmr.2016.01.015, 2016.

Arputharaj, D. S., Hathwar, V. R., Guru Row, T. N. and Kumaradhas, P.: Topological Electron Density Analysis and Electrostatic Properties of Aspirin: An Experimental and Theoretical Study, Cryst. Growth Des., 12(9), 4357–4366, doi:10.1021/cg300269n, 2012.

Barlow, M. J., Clough, S., Horsewill, A. J. and Mohammed, M. A.: Rotational frequencies of methyl group tunneling, Solid State Nucl. Magn. Reson., 1(4), 197–204, doi:10.1016/S0926-2040(10)80004-9, 1992.

Bertini, I., Luchinat, C., Parigi, G. and Pierattelli, R.: NMR spectroscopy of paramagnetic metalloproteins, ChemBioChem, 6(9), 1536–1549, doi:10.1002/cbic.200500124, 2005.

Bode, B. E., Thamarath, S. S., Gupta, K. B. S. S., Alia, A., Jeschke, G. and Matysik, J.: The Solid-State Photo-CIDNP Effect and Its Analytical Application, in Hyperpolarization methods in NMR spectroscopy, edited by L. Kuhn, pp. 105–121, Springer., 2013.

Dietrich, C., Wissel, J., Knoche, J., Lorenz, O. and Matysik, J.: Simple device for dissolution and sample transfer for applications in spin-hyperpolarization, Mol. Phys., 8976, 1–5, doi:10.1080/00268976.2018.1550224, 2018.

Duckett, S. B. and Mewis, R. E.: Application of para hydrogen induced polarization techniques in NMR spectroscopy and imaging, Acc. Chem. Res., 45(8), 1247–1257, doi:10.1021/ar2003094, 2012.

https://doi.org/10.5194/mr-2021-51
Preprint. Discussion started: 15 July 2021

Open Access MAGNETIC RESONANCE Discussions

1 Dumez, J. N., Vuichoud, B., Mammoli, D., Bornet, A., Pinon, A. C., Stevanato, G., Meier, B., Bodenhausen,
2 G., Jannin, S. and Levitt, M. H.: Dynamic Nuclear Polarization of Long-Lived Nuclear Spin States in Methyl
3 Groups, J. Phys. Chem. Lett., 8(15), 3549–3555, doi:10.1021/acs.jpclett.7b01512, 2017.

4 Faber, A., Lemke, A., Spangenberg, B. and Bolte, M.: Three hydrohalogenides of organic nitrogen bases,
5 Acta Crystallogr. Sect. C Cryst. Struct. Commun., 55(12), IUC9900156, doi:10.1107/S0108270199098261,
6 1999.

7 Galigné, J. L., Mouvet, M. and Falgueirettes, J.: Nouvelle détermination de la structure cristalline de l'acétate
8 de lithium dihydraté CH3COOLi.2H2O, Acta Crystallogr. Sect. B Struct. Crystallogr. Cryst. Chem., 26(4),
9 368–372, doi:10.1107/S0567740870002418, 1970.

10 Gangu, K. K., Maddila, S., Mukkamala, S. B. and Jonnalagadda, S. B.: A review on contemporary Metal-
11 Organic Framework materials, Inorganica Chim. Acta, 446, 61–74, doi:10.1016/j.ica.2016.02.062, 2016.

12 Gonzalez-Nelson, A., Coudert, F. X. and van der Veen, M. A.: Rotational dynamics of linkers in metal–
13 organic frameworks, Nanomaterials, 9(3), doi:10.3390/nano9030330, 2019.

14 Gueron, M.: Nuclear relaxation in macromolecules by paramagnetic ions: a novel mechanism, J. Magn.
15 Reson., 19(1), 58–66, doi:10.1016/0022-2364(75)90029-3, 1975.

16 Gutsche, C. D.: "Properties of the Calixarenes from p-tert-Butylphenol," J. Am. Chem. Soc., Ryu, E., (8),
17 3782–3792, doi:10.1021/ja00403a028, 1981.

18 Halse, M. E.: Perspectives for hyperpolarisation in compact NMR, TrAC - Trends Anal. Chem.,
19 doi:10.1016/j.trac.2016.05.004, 2016.

20 Haupt, J.: A new effect of dynamic polarization in a solid obtained by rapid change of temperature, Phys.
21 Lett., 38A(6), 389–390, 1972.

22 Haupt, J.: Experimental Results on the Dynamic Polarisation in a Solid by Variation of Temperature, Z.
23 Naturforsch., 28a, 98–104, 1973.

24 Hollenbach, J., Anger, B. and Matysik, J.: Chapter 9. Probing Exchange and Diffusion in Confined Systems
25 by 129Xe NMR Spectroscopy, in Diffusion NMR of Confined Systems: Fluid Transport in Porous Solids and
26 Heterogeneous Materials, edited by R. Valiullin, pp. 294–317., 2016.

27 Horsewill, A. J.: Quantum tunnelling aspects of methyl group rotation studied by NMR, Prog. Nucl. Magn.
28 Reson. Spectrosc., 35(4), 359–389, doi:10.1016/S0079-6565(99)00016-3, 1999.

29 Icker, M.: Hyperpolarisation in fester und flüssiger Phase und ihr Potential in der hochauflösenden
30 magnetischen Kernresonanz-Spektroskopie, Leipzig University., 2013.

31 Icker, M. and Berger, S.: Unexpected multiplet patterns induced by the Haupt-effect, J. Magn. Reson., 219,
32 1–3, doi:10.1016/j.jmr.2012.03.021, 2012.

33 Icker, M., Fricke, P., Grell, T., Hollenbach, J., Auer, H. and Berger, S.: Experimental boundaries of the
34 quantum rotor induced polarization (QRIP) in liquid state NMR, Magn. Reson. Chem., 51(12), 815–820,
35 doi:10.1002/mrc.4021, 2013.

36 Johnston, D. H. and Crather, H. M.: 2,5-Dimethyl-1,3-dinitrobenzene, Acta Crystallogr. Sect. E Struct.
37 Reports Online, 67(9), o2276–o2277, doi:10.1107/S1600536811031424, 2011.

38 Khan, A. H., Barth, B., Hartmann, M., Haase, J. and Bertmer, M.: Nitric Oxide Adsorption in MIL-100(Al)
39 MOF Studied by Solid-State NMR, J. Phys. Chem. C, 122(24), 12723–12730, doi:10.1021/acs.jpcc.8b01725,
40 2018.

41 Khazaei, S. and Sebastiani, D.: Methyl rotor quantum states and the effect of chemical environment in
42 organic crystals: γ-picoline and toluene, J. Chem. Phys., 145(23), 234506, doi:10.1063/1.4971380, 2016.

43 Khazaei, S. and Sebastiani, D.: Tunneling of coupled methyl quantum rotors in 4-methylpyridine : Single rotor
44 potential versus coupling interaction Tunneling of coupled methyl quantum rotors in 4-methylpyridine : Single
45 rotor potential versus coupling interaction, J. Chem. Phys., 147(194303), 1–9, 2017.

https://doi.org/10.5194/mr-2021-51
Preprint. Discussion started: 15 July 2021

Open Access MAGNETIC RESONANCE Discussions

1 Kiryutin, A. S., Korchak, S. E., Ivanov, K. L., Yurkovskaya, A. V. and Vieth, H. M.: Creating long-lived spin
2 states at variable magnetic field by means of photochemically induced dynamic nuclear polarization, J. Phys.
3 Chem. Lett., 3(13), 1814–1819, doi:10.1021/jz3005046, 2012.

4 Kiryutin, A. S., Sauer, G., Yurkovskaya, A. V., Limbach, H. H., Ivanov, K. L. and Buntkowsky, G.:
5 Parahydrogen Allows Ultrasensitive Indirect NMR Detection of Catalytic Hydrogen Complexes, J. Phys.
6 Chem. C, 121(18), 9879–9888, doi:10.1021/acs.jpcc.7b01056, 2017.

7 Kjeldsen, C., Ardenkjær-Larsen, J. H. and Duus, J. O.: Discovery of Intermediates of lacZ β-Galactosidase
8 Catalyzed Hydrolysis Using dDNP NMR, J. Am. Chem. Soc., 140(8), 3030–3034, doi:10.1021/jacs.7b13358,
9 2018.

10 Köckenberger, W. and Matysik, J.: Magnetic resonance: Hyperpolarization methods and applications in
11 NMR, in Encyclopedia of Spectroscopy and Spectrometry, 2nd edition, edited by J. C. Lindon, pp. 963–970,
12 Elsevier., 2010.

13 Korchak, S. E., Ivanov, K. L., Yurkovskaya, A. V. and Vieth, H. M.: Para-hydrogen induced polarization in
14 multi-spin systems studied at variable magnetic field, Phys. Chem. Chem. Phys., 11(47), 11146–11156,
15 doi:10.1039/b914188j, 2009.

16 Kovtunov, K. V., Pokochueva, E. V., Salnikov, O. G., Cousin, S. F., Kurzbach, D., Vuichoud, B., Jannin, S.,
17 Chekmenev, E. Y., Goodson, B. M., Barskiy, D. A. and Koptyug, I. V.: Hyperpolarized NMR Spectroscopy: d
18 -DNP, PHIP, and SABRE Techniques, Chem. - An Asian J., 13(15), 1857–1871,
19 doi:10.1002/asia.201800551, 2018.

20 Kuc, A., Enyashin, A. and Seifert, G.: Metal-organic frameworks: Structural, energetic, electronic, and
21 mechanical properties, J. Phys. Chem. B, 111(28), 8179–8186, doi:10.1021/jp072085x, 2007.

22 Kwon, H. T., Jeong, H. K., Lee, A. S., An, H. S. and Lee, J. S.: Heteroepitaxially Grown Zeolitic Imidazolate
23 Framework Membranes with Unprecedented Propylene/Propane Separation Performances, J. Am. Chem.
24 Soc., 137(38), 12304–12311, doi:10.1021/jacs.5b06730, 2015.

25 Li, Q., Zaczek, A. J., Korter, T. M., Zeitler, J. A. and Ruggiero, M. T.: Methyl-rotation dynamics in metal–
26 organic frameworks probed with terahertz spectroscopy, Chem. Commun., 54(45), 5776–5779,
27 doi:10.1039/C8CC02650E, 2018.

28 Lilly Thankamony, A. S., Wittmann, J. J., Kaushik, M. and Corzilius, B.: Dynamic nuclear polarization for
29 sensitivity enhancement in modern solid-state NMR, Prog. Nucl. Magn. Reson. Spectrosc., 102–103, 120–
30 195, doi:10.1016/j.pnmrs.2017.06.002, 2017.

31 Ludwig, C., Saunders, M., Marin-Montesinos, I. and Günther, U. L.: Quantum rotor induced
32 hyperpolarization, Proc. Natl. Acad. Sci. U. S. A., 107(24), 10799–10803, doi:10.1073/pnas.0908421107,
33 2010.

34 Meersmann, T. and Brunner, E.: Hyperpolarized Xenon-129 Magnetic Resonance, edited by T. Meersmann
35 and E. Brunner, Royal Society of Chemistry, Cambridge., 2015.

36 Milani, J., Vuichoud, B., Bornet, A., Miéville, P., Mottier, R., Jannin, S. and Bodenhausen, G.: A magnetic
37 tunnel to shelter hyperpolarized fluids, Rev. Sci. Instrum., 86(2), doi:10.1063/1.4908196, 2015.

38 Moggach, S. A., Wharmby, M. T., Wright, P. A. and Parsons, S.: Opening the Gate : Framework Flexibility in
39 ZIF-8 Explored by Experiments and Simulations, J. Am. Chem. Soc., 133, 8900–8902,
40 doi:10.1021/ja202154j, 2011.

41 Morris, W., Stevens, C. J., Taylor, R. E., Dybowski, C., Yaghi, O. M. and Garcia-Garibay, M. A.: NMR and X-
42 ray study revealing the rigidity of zeolitic imidazolate frameworks, J. Phys. Chem. C, 116(24), 13307–13312,
43 doi:10.1021/jp303907p, 2012.

44 Ni, Q. Z., Daviso, E., Can, T. V., Markhasin, E., Jawla, S. K., Swager, T. M., Temkin, R. J., Herzfeld, J. and
45 Griffin, R. G.: High Frequency Dynamic Nuclear Polarization, Acc. Chem. Res., 46(9), 1933–1941,
46 doi:10.1021/ar300348n, 2013.

47 Norquay, G., Collier, G. J., Rao, M., Stewart, N. J. and Wild, J. M.: Xe 129 -Rb Spin-Exchange Optical

https://doi.org/10.5194/mr-2021-51
Preprint. Discussion started: 15 July 2021

Open Access MAGNETIC RESONANCE Discussions

Pumping with High Photon Efficiency, Phys. Rev. Lett., 121(15), 153201, doi:10.1103/PhysRevLett.121.153201, 2018.

Ohms, U., Guth, H., Treutmann, W., Dannöhl, H., Schweig, A. and Heger, G.: Crystal structure and charge density of 4-methylpyridine (C 6 H 7 N) at 120 K, J. Chem. Phys., 83(1), 273–279, doi:10.1063/1.449820, 1985.

Prager, M. and Heidemann, A.: ChemInform Abstract: Rotational Tunneling and Neutron Spectroscopy: A Compilation, ChemInform, 29(11), no-no, doi:10.1002/chin.199811329, 2010.

van der Putten, D., Diezemann, G., Fujara, F. and Sillescu, H.: Methyl Group Dynamics in α-Crystallized Toluene as Studied by 2H-Spin Lattice Relaxation, in 25th Congress Ampere on Magnetic Resonance and Related Phenomena, pp. 520–521, Springer Berlin Heidelberg, Berlin, Heidelberg., 1990.

Rehm, M., Frank, M. and Schatz, J.: Water-soluble calixarenes-self-aggregation and complexation of noncharged aromatic guests in buffered aqueous solution, Tetrahedron Lett., 50(1), 93–96, doi:10.1016/j.tetlet.2008.10.089, 2009.

Reilly, A. M. and Tkatchenko, A.: Role of Dispersion Interactions in the Polymorphism and Entropic Stabilization of the Aspirin Crystal, Phys. Rev. Lett., 113(5), 055701, doi:10.1103/PhysRevLett.113.055701, 2014.

Roy, S. S., Levitt, M. H., Dumez, J.-N., Mamone, S., Hill-Cousins, J. T., Stevanato, G., Brown, R. C. D., Meier, B., Håkansson, P. and Pileio, G.: Long-Lived Nuclear Spin States in Methyl Groups and Quantum-Rotor-Induced Polarization, J. Am. Chem. Soc., 135(50), 18746–18749, doi:10.1021/ja410432f, 2013.

Sosnovsky, D. V., Lukzen, N. N., Vieth, H.-M., Jeschke, G., Gräsing, D., Bielytskyi, P., Matysik, J. and Ivanov, K. L.: Magnetic field and orientation dependence of solid-state CIDNP, J. Chem. Phys., 150(9), 094105, doi:10.1063/1.5077078, 2019.

Tarasi, S., Tehrani, A. A. and Morsali, A.: The effect of methyl group functionality on the host-guest interaction and sensor behavior in metal-organic frameworks, Sensors Actuators, B Chem., 305, 127341, doi:10.1016/j.snb.2019.127341, 2020.

Tian, Y. Q., Zhao, Y. M., Chen, Z. X., Zhang, G. N., Weng, L. H. and Zhao, D. Y.: Design and generation of extended zeolitic metal-organic frameworks (ZMOFs): Synthesis and crystal structures of zinc(II) imidazolate polymers with zeolitic topologies, Chem. - A Eur. J., 13(15), 4146–4154, doi:10.1002/chem.200700181, 2007.

Ullah, Z., Bustam, M. A., Man, Z., Muhammad, N. and Khan, A. S.: Synthesis, characterization and the effect of temperature on different physicochemical properties of protic ionic liquids, RSC Adv., 5(87), 71449–71461, doi:10.1039/C5RA07656K, 2015.

Vega, A. J. and Fiat, D.: Nuclear relaxation processes of paramagnetic complexes - The slow-motion case, Mol. Phys., 31(2), 347–355, doi:10.1080/00268977600100261, 1976.

Walker, T. G.: Fundamentals of spin-exchange optical pumping, J. Phys. Conf. Ser., 294(1), doi:10.1088/1742-6596/294/1/012001, 2011.

Wang, J., Chen, S.-B., Wang, S.-G. and Li, J.-H.: A Metal-Free and Ionic Liquid-Catalyzed Aerobic Oxidative Bromination in Water, Aust. J. Chem., 68(3), 513, doi:10.1071/CH14161, 2015.

Wang, Y. and Yan, H.: Crystal structure of (E)- N ′-(3,4-difluorobenzylidene)-4-methylbenzenesulfonohydrazide, Acta Crystallogr. Sect. E Crystallogr. Commun., 71(10), o761–o761, doi:10.1107/S2056989015016205, 2015.

Wang, Z. J., Ohliger, M. A., Larson, P. E. Z., Gordon, J. W., Bok, R. A., Slater, J., Villanueva-Meyer, J. E., Hess, C. P., Kurhanewicz, J. and Vigneron, D. B.: Hyperpolarized 13C MRI: State of the Art and Future Directions, Radiology, 291(2), 273–284, doi:10.1148/radiol.2019182391, 2019.

Zhou, W., Wu, H., Udovic, T. J., Rush, J. J. and Yildirim, T.: Quasi-Free Methyl Rotation in Zeolitic Imidazolate Framework-8, J. Phys. Chem. A, 112, 12602–12606, 2008.